Aerospace Science and Technology 42 (2015) 187–195

Contents lists available at ScienceDirect

Aerospace Science and Technology

www.elsevier.com/locate/aescte

Simplified brain storm optimization approach to control parameter optimization in F/A-18 automatic carrier landing system

Junnan Li, Haibin Duan *

State Key Laboratory of Virtual Reality Technology and Systems, School of Automation Science and Electrical Engineering, Beihang University, Beijing 100191, PR China

ARTICLE INFO

Article history:
Received 3 September 2014
Received in revised form 18 January 2015
Accepted 20 January 2015
Available online 23 January 2015

Keywords:
Automatic carrier landing system (ACLS)
Brain Storming Optimization (BSO)
Parameter optimization

ABSTRACT

The design of automatic carrier landing system is a crucial technique for carrier-based aircraft, since it facilitates landing of aircraft on carriers in various severe weather conditions, such as low visibility, heavy wind and rough sea conditions, which can hardly be achieved by manual control. In this paper, a novel method of optimizing the control parameters in the automatic carrier landing system of F/A-18A is developed, which is based on simplified Brain Storming Optimization (BSO) algorithm. The gains in the inner loop are optimized by fitting the frequency response curve of the closed-loop system with a desired frequency response curve. The control parameters in the autopilot and auto-throttle control module are optimized by minimizing a set of objective functions defined in the time domain. Comparative experiments are conducted to verify the effectiveness of our proposed method.

1. Introduction

Carrier-based aircraft are important combat forces in modern navy. The ability to land safely on carriers in all weather conditions is a big challenge for all carrier-based aircraft. In manual landing operations, the pilots are under great pressure and accidents often occur if the weather condition is severe. Automatic Carrier Landing System (ACLS) is developed to relieve the pilot and help the aircraft achieve accurate sink rate and touchdown position in various conditions of sea state, visibility and air turbulence.

Usually, ACLS system consists of five components: flight control system, throttle control system, inertial navigation sensors, data link and the shipboard radar system [29]. The shipboard radar system tracks the position of the aircraft and computes the H-dot command or the pitch angle command. Afterwards, the command is transmitted to the aircraft by data link. The flight control system and throttle control system are used to manipulate the aircraft to follow the H-dot command or the pitch angle command to track the glide slope accurately. The control system is composed of the inner loop, the autopilot, and Approach Power Compensation System (APCS). The inner loop is similar to the conventional Control Augmentation System (CAS) used in other flight conditions, which increases the stability and the handling quality of the aircraft. The autopilot is used to follow the H-dot command or the pitch angle command, and create input signal for the inner loop. In the history of ACLS, two types of autopilot systems have been used. For instance, the ACLS of F-4J jet adopts the pitch angle command autopilot, while the ACLS of F/A-18A jet adopts H-dot command autopilot [13,20]. The H-dot command autopilot is proven to be more effective in alleviating the influence of air turbulence in automatic landings [30]. As a consequence, it is seen as a better option for advanced carrier-based aircraft. The APCS is used to maintain a constant velocity and angle of attack during the landing process [34]. The aircraft will rotate and cannot achieve an accurate flight path angle without a constant angle of attack. The study in Ref. [5] gave a detailed analysis of the APCS used in the US navy.

In additional to the traditional PID controller, the researchers have also investigated using more advanced controllers in ACLS. In Ref. [24], the authors designed a fuzz logic controller for the ACLS of F/A-18. The robust control design of ACLS was studied in Refs. [26] and [6]. A comparison of neural, fuzzy, evolutionary, and adaptive approaches for carrier landing control was given in Ref. [25].

After determining the structure of the control system, the designers have to adjust the parameters used in the control law to achieve the best control performance. However, the process of adjusting the control parameters is difficult and tedious even for designers with much experience. One major difficulty of the problem is that the number of the control parameters to be adjusted is relatively large, and an experienced designer often can only adjust one or two of the parameters at one time. Most of the time, the best control performance under the given control structure cannot

* Corresponding author. Tel.: +86 10 82317318.
E-mail address: hbduan@buaa.edu.cn (H. Duan).

http://dx.doi.org/10.1016/j.ast.2015.01.017
1270-9638/

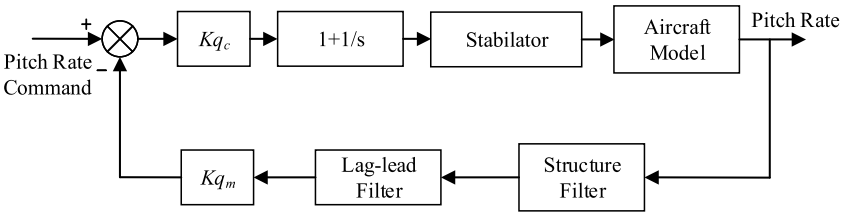

Fig. 1. The block diagram of the inner loop in ACLS.

be achieved. Aviation engineers have come up with many methods to optimize the parameters used in the flight control systems [17,16,19].

Recently, many researchers turn to bio-inspired optimization algorithms to solve the control parameter optimization problem [2,3,1,11,7]. Bio-inspired optimization algorithm is a flourishing field today. Some bio-inspired optimization methods like Genetic Algorithm (GA), Particle Swarm Optimization (PSO) and Gravitational Search Algorithm (GSA) have been successfully applied to solve optimization problems in various fields [18,10,15,8]. The study in Ref. [14] used GA to optimize the feedback gains in two flight control systems. In Ref. [27], GA was applied to optimize the adaptive leading edge of an airfoil. In recent years, many new bio-inspired optimization algorithms were proposed. Among them, Brain Storming Optimization (BSO) is a promising method. BSO was proposed by Shi in 2011, which mimics the brainstorming process of a group of people working together to come up with new ideas to solve a difficult problem [22]. Intuitively, Shi thought the collective behavior of human beings should be superior to that of insects or animals, since human beings are the most intelligent creature on this planet. In Ref. [23], Shi proposed an improved model of BSO, and gave a detailed analysis of the algorithm. In Ref. [33], Zhou studied adapting the step-size of BSO according to the dynamic range of individuals on each dimension. The values of the parameters used in BSO are investigated in Ref. [32], and the effect of the solution clustering in BSO is analyzed in Ref. [4]. Other researchers also conducted much work to make BSO more effective, and applied this algorithm to solve several real-world problems [9,28,21,12].

In this study, we make some simplifications to the basic BSO, and name the new algorithm Simplified Brain Storming Optimization (SBSO). To illustrate the effectiveness of SBSO, we apply both BSO and SBSO to a set of benchmark functions. Therefore, SBSO is applied to optimize the control parameters in the F/A-18A ACLS. The gains in the inner loop are optimized by fitting the frequency response curve of the closed-loop system with a desired frequency response curve. The control parameters in the H-dot command autopilot and APCS are optimized by minimizing a set of objective functions defined in the time domain.

The remainder of this paper is organized as follows. In Section 2, we briefly introduce the longitudinal model of F/A-18A, and descriptions of the main components of ACLS including the inner loop, the H-dot autopilot loop and APCS can also be seen in this section. A concise introduction of the basic BSO and the detail of SBSO algorithm can be seen in Section 3. In Section 4, the control parameter optimization method based on SBSO is introduced, followed by experimental simulation and result analysis in Section 5. Finally, conclusions are given in the last section.

2. The F/A-18A automatic carrier landing system

2.1. The longitudinal model of F/A-18A

In this work, the longitudinal small turbulence dynamic model of F/A-18A is considered, the model is described in the following:

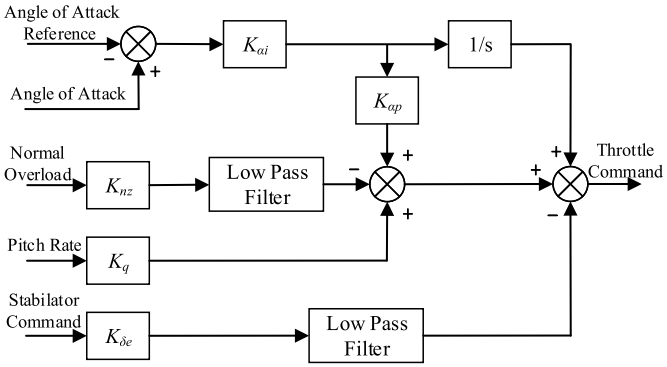

Fig. 2. The block diagram of the APCS.

$$\begin{cases} \dot{x} = Ax + Bu \\ y = Cx + Du \end{cases}$$

$$x = (\Delta u/V_0, \Delta\alpha, \Delta\theta, \Delta q, \Delta h/V_0)^T$$

$$u = (\Delta\delta_s, \Delta\delta_{LEF}, \Delta\delta_{PL})^T$$

$$y = (\Delta h, \Delta\gamma, \Delta n_z/V_0, \Delta\alpha, \Delta u, \Delta\theta, \Delta q)^T \quad (1)$$

where, $\Delta u, \Delta\alpha, \Delta\theta, \Delta q, \Delta\gamma, \Delta n_z, \Delta h$ are the variation of velocity, angle of attack, pitch angle, pitch rate, flight path angle, normal acceleration and height respectively. $\Delta\delta_s, \Delta\delta_{LEF}, \Delta\delta_{PL}$ are the deflection of stabilator, the deflection of leading-edge flap and the output of throttle respectively. The trim values of the states are: $V_0 = 69.96$ m/s, $\gamma_0 = -3.5$ deg and $\alpha_0 = 8.1$ deg.

2.2. Control system description

The control structure of the inner loop used in the ACLS of F/A-18A is designed to achieve rapid dynamic response to the vertical rate command. The block diagram of the inner loop is shown in Fig. 1. The pitch rate signal is taken as the feedback signal. In the feedback loop, a structure filter is used to eliminate the structure mode oscillation which is sensed by the rate gyroscope. The lag-lead filter is used to provide necessary lead response for the system to achieve high flight path bandpass. In the forward path, a high integrator gain is applied to achieve a flat low-frequency response.

The aircraft cannot trace a landing path precisely without a constant angle of attack and velocity, to this end, the APCS is applied to maintain a constant angle of attack and velocity during the landing process. APCS uses angle of attack α and normal overload n_z as the main feedback signals. The block diagram of APCS is shown in Fig. 2, the APCS maintains a constant α, and consequently a constant velocity can be achieved. The pitch rate feedback is used to increase the damping ratio of the system. The stabilator command signal is introduced into the APCS feedback signal to alleviate the impact of the stabilator deflection. The filers are used to eliminate the high frequency noise in n_z signal and the stabilator command. There are other feedback signals used in the actual F/A-18A APCS, such as the roll angle and the crossover com-

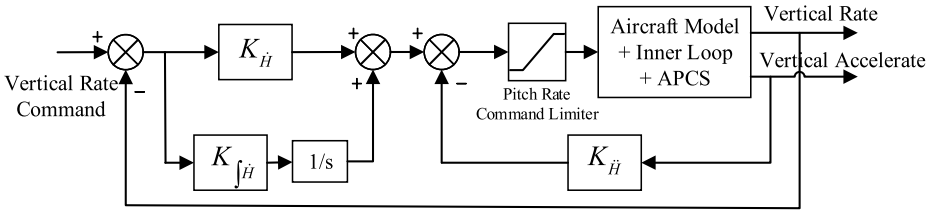

Fig. 3. The block diagram of H-dot autopilot in ACLS.

mand from the aileron to the stabilator. However, for the purpose of simplicity, they are not considered in this work.

The H-dot command autopilot is used in this work, which has been proved to have a better capability to alleviate the influence of the air turbulence than the pitch angle command autopilot. The vertical rate of the aircraft can be computed by $\dot{H} = V \sin\gamma$. From the equation we can see that, the control of the vertical rate is equivalent to the control of the flight path angle. On the contrast, the pitch angle command autopilot controls the pitch angle directly, and then influences the flight path angle indirectly. The block diagram of the H-dot command autopilot is shown in Fig. 3. A vertical acceleration signal is used in the feedback loop to increase the damping ratio of the system. The pitch rate command limit is usually set to 3 deg/s.

3. Simplified brain storm optimization algorithm

3.1. The basic brain storm optimization algorithm

The BSO algorithm is inspired by human beings' brainstorming process to solve specific problems. Each idea in BSO represents an individual in the searching space. The first step of the brainstorming process is to gather some people with different backgrounds and then divide them into several groups. In each group, a facilitator is elected to supervise the new idea generation process and enforce the group members to obey the rules of brainstorming. In BSO, this step is imitated by dividing the ideas into different clusters, and the idea with the best fitness value in each cluster is taken as the cluster center. The second step in brainstorming process is to generate new ideas. The new ideas can be created within each group, or created by exchanging ideas with other groups. In BSO, the new idea generating step is mimicked by adding a random number to each dimension of an old idea. The old idea is obtained by choosing one idea randomly from one cluster, or by combining two ideas chosen randomly from two clusters. The clusters with larger idea number are more likely to be chosen. In each cluster, the cluster center has a higher possibility to be chosen than other ordinary ideas. In brainstorming process, group members' mind-set may be narrowed occasionally, and useful new ideas become more and more difficult to be thought out. In such situation, a random object will be chosen to motivate people's creativity, and then the group members start to think about ideas related to the object. In BSO, this mechanism is mimicked by replacing the cluster center with a randomly generated idea with a certain possibility. This helps the algorithm to explore more potential solutions.

BSO works as follows:

Step 1: Generate n ideas X_i randomly and evaluate them by the cost function $f(X_i)$.

Step 2: Divide n ideas into m clusters using k-means clustering method. In each cluster, chose the ideas with the best cost function value as the cluster center:

$$X_c(k) = \arg\min f\big(X_i(k)\big), \quad k = 1, 2, \ldots, m \tag{2}$$

where $X_i(k)$ means the idea belongs to the k-th cluster.

Step 3: Select a cluster randomly. Generate a random number from 0 to 1, if $rand < p_{5a}$, replace the cluster center of the selected cluster with a randomly generated idea X_{rand}.

Step 4: Generate an idea X_{old}. Generate a random number from 0 to 1.

a) If $rand < p_b$, select one idea from one cluster to generate X_{old}.

The clusters with larger idea number are more likely to be selected. N denotes the number of ideas in each cluster, the possibility for the k-th cluster to be selected is:

$$p_{6bi}(k) = \frac{N(k)}{\sum_{l=1}^{m} N(l)}, \quad k = 1, 2, \ldots, m \tag{3}$$

$X_c(k)$ denotes the cluster center of the selected cluster. Generate a random number $rand$, if $rand < p_{6biii}$, take the cluster center as X_{old}, i.e. $X_{old} = X_c(k)$. Otherwise, randomly chose an idea $X_i(k)$ from the selected cluster as X_{old}, i.e. $X_{old} = X_i(k)$.

b) If $rand > p_b$, select two ideas from two clusters respectively, and combine them to generate X_{old}.

Randomly select two clusters k_1 and k_2. Generate a random number $rand$, if $rand < p_{6c}$, then take the combination of the two selected cluster centers as X_{old}, i.e. $X_{old} = R \cdot X_c(k_1) + (1 - R)X_c(k_2)$, where R is a random number between 0 and 1. Otherwise, randomly chose two ideas $X_i(k_1)$ and $X_j(k_2)$ from the two selected clusters k_1 and k_2 respectively, take the combination of $X_i(k_1)$ and $X_j(k_2)$ as X_{old}, i.e. $X_{old} = R \cdot X_i(k_1) + (1 - R)X_j(k_2)$.

Step 5: Generate a new idea X_{new} by adding a random value to each dimension of X_{old} according to:

$$X_{new}^i = X_{old}^i + \xi \times N(\mu, \sigma) \tag{4}$$

where $N(\mu, \sigma)$ is a random value with Gaussian distribution, μ is the mean value and σ is the variance. i represents the ith dimension of the vector. ξ is an alterable factor which decreases as the iteration goes:

$$\xi = \log\operatorname{sig}\left(\frac{0.5Nc_{\max} - Nc}{K}\right) \times rand \tag{5}$$

where $Nc_{\max}$ is the maximum iteration number and Nc is the current iteration. K is a factor which determines the slope of the log sig function. The factor ξ strengthens the global searching capability at the early stage of the algorithm and strengthens the local searching capability at the later stage.

Step 6: Crossover $X(i)$ and X_{new} (similar to the crossover operation in GA), and generate two more new ideas, the best one in the four ideas is kept as the new idea into the next iteration.

Step 7: If N new ideas are generated, go to Step 8, otherwise, go back to Step 5.

Step 8: Check the stopping criteria. If $Nc < Nc_{\max}$, go back to Step 2, otherwise, stop the algorithm and output the result.

3.2. The simplified brain storm optimization algorithm

The basic BSO applies k-means method to divide the ideas into several clusters. However, the k-means method itself is an iterative algorithm, which requires considerable time to converge. Zhan utilized a Simple Grouping Method (SGM) in BSO to replace the k-means method [31]. SGM selected M individuals as the seeds of the M clusters randomly, and assigned the other individuals into the M clusters according to the distance between each individual and each seed. Compared with k-means method, SGM is not an accurate clustering method. Fortunately, an accurate clustering method is not necessary in BSO, so SGM is a good option for BSO since it can reduce the calculation burden of the algorithm greatly. In this work, we also utilize SGM as the clustering method.

In addition to utilize SGM in place of the k-means method, we introduce another modification to the basic BSO. That is simplifying the X_{old} generating operation. As is described in the previous section, in the basic BSO, there are totally four ways to generate X_{old}, this makes the algorithm complicated. The algorithm must generate several random numbers to see which criteria is satisfied and then determine which operation is conducted. Parameters p_b, p_{6biii} and p_{6c} must be well tuned before running the algorithm to achieve a good performance. This increases the burden of the users. We simplify the X_{old} generating step by always using one operation to generate X_{old}, which is taking the combining of the two ideas randomly selected from two clusters as X_{old}:

$$X_{old} = R \cdot X_i(k_1) + (1 - R)X_j(k_2) \tag{6}$$

In this way, Step 4 is greatly simplified. Since the cluster centers are no longer special in the X_{old} generating operation, it's not necessary to select a cluster center in each cluster in Step 2. As a consequence, Step 3 can be omitted, too.

In addition to reducing the complicity of the algorithm, our method may have another advantage. In the X_{new} generating operation, noise is added to X_{old}, but the maximum value of the noise does not change when the scale of the searching space changes. If X_{old} is an idea which already exists in the population, and the searching space is relatively large, while the maximum value of the noise is relatively small, the basic BSO may converge slowly in the early stage of the algorithm. By conducting more operations of combining two ideas selected from different clusters, a better idea is more likely to be found, so SBSO is expected to have a faster convergence rate. The flowchart of SBSO is shown in Fig. 4.

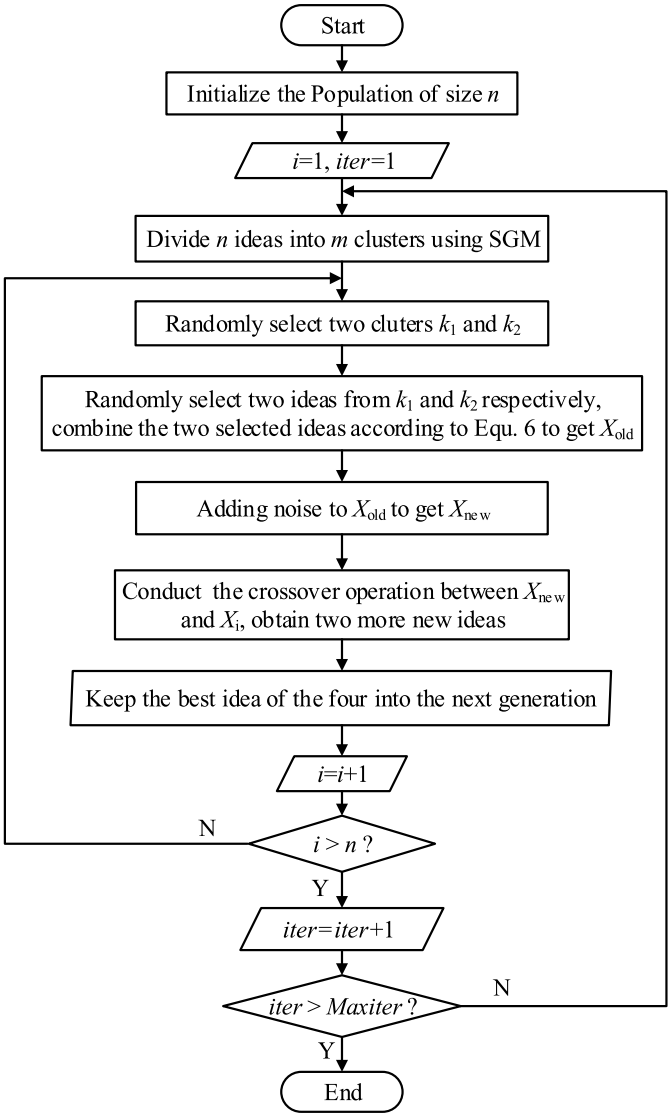

Fig. 4. Flowchart of SBSO.

4. Control parameter optimization based on SBSO

Adjusting the control parameters manually is a tedious and difficult work, and the best control performance under the given configuration often cannot be achieved. The process of optimizing the control parameters can be seen as a constrained multi-objective optimization problem. In this work, we use an optimization method based on SBSO to optimize the control parameters in the inner loop, the autopilot loop and the APCS.

4.1. Inner loop optimization

The control structure of the inner loop is shown in Fig. 1. The gains in the inner loop are optimized by fitting the frequency response curve of the closed-loop system with a desired frequency response curve. In Ref. [29], the authors gave the actual frequency response curve of the F/A-18A inner loop, and the desired frequency response curve used in this paper is taken from that literature, as is shown in Fig. 5.

The features of the desired frequency response curve are able to ensure the time domain response requirements of the system.

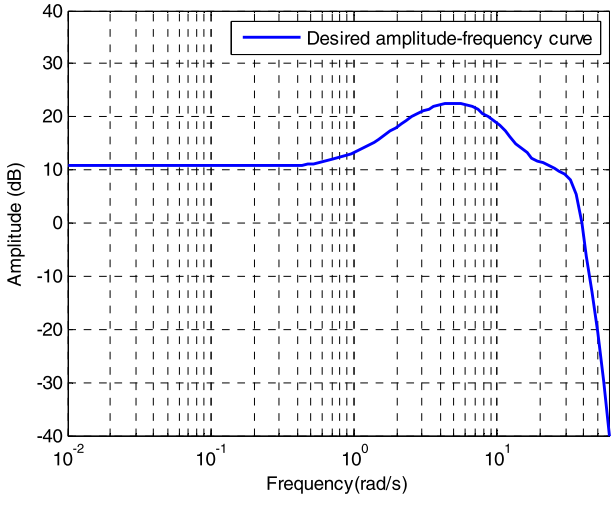

Fig. 5. The desired frequency response curve.

Table 1
Parameter used in BSO and SBSO.

Method	Population size	Cluster number	Max iteration	p_{5a}	p_{6b}	p_{6biii}	p_{6c}	k	μ	σ
BSO	100	5	2000	0.2	0.8	0.4	0.5	20	0	1
SBSO	100	5	2000	–	–	–	–	20	0	1

The higher amplitude between the frequency range 2–30 rad/s in the desired frequency response curve ensures that the inner loop of the controlled system has a high band pass to the pitch rate command. The structure mode oscillation sensed by the rate gyroscope is around the frequency point 60 rad/s. The desired frequency response curve has a very low amplitude around 60 rad/s, this feature can help reduce the influence of the structure mode oscillation. In addition, the flat low-frequency response in the desired frequency response curve ensures the steady accuracy of the system.

The cost function of the optimization problem is defined as the error between the frequency response curve of the inner loop and the desired frequency response curve plus a constraint penalty,

$$f(X) = \sum_{i=1}^{100} \left(G(j\omega_i) - G_d(j\omega_i)\right)^2 + constraint \tag{7}$$

where ω_1–ω_{100} are one hundred frequency points selected uniformly in the logarithmic frequency coordinate between 0.01 to 60 rad/s. $G(j\omega)$ is the frequency response curve of the inner loop, while $G_d(j\omega)$ is the desired frequency response curve. If the magnitude margin constraint or the phase margin constraint of the open loop is violated, a constraint penalty is added to the cost function. The magnitude margin constraint and the phase margin constraint are set as 6 dB and 40 deg.

The lag-lead filter used in Fig. 1 is in the form of:

$$G_{lag\text{-}lead}(s) = \frac{s+1}{Ts+1} \tag{8}$$

Since the lag-lead filter affects the shape of the frequency response curve significantly, parameter T also need to be optimized. In summary, there are three parameters to be optimized in the inner loop:

$$X = [K_{qm}, K_{qc}, T] \tag{9}$$

4.2. APCS and autopilot loop optimization

APCS is used to maintain a constant angle of attack during the landing process, while the autopilot loop is used to follow a vertical rate command. The two parts couple with each other, so we optimize the control parameters in APCS and the autopilot loop simultaneously. A constant reference signal is given to APCS, the control parameters in APCS are adjusted to ensure the attack angle to be as constant as possible during the landing. A vertical rate command is given to the system, and the aircraft is supposed to track the command with a rapid rise time, a minimum overshoot and a high steady accuracy. In total, there are eight control parameters to be optimized in the autopilot plus the APCS:

$$X = [K_{ai}, K_{ap}, K_{nz}, K_q, K_{\delta e}, K_{\dot{H}}, K_{\ddot{H}}, K_{\int \dot{H}}] \tag{10}$$

The objective functions of the rise time, the overshoot and the steady accuracy of the vertical rate response to the command are defined in the time domain as follows:

$$\text{Rise time:} \quad \begin{cases} f_1(X) = t_2 - t_1 \\ \dot{H}(t_1) = 0.1\dot{H}_c,\ \dot{H}(t_2) = 0.9\dot{H}_c \end{cases}$$

$$\text{Overshoot:} \quad f_2(X) = \max_{t>0} \left| \frac{\dot{H}(t)}{\dot{H}_c} \right|$$

$$\text{Steady accuracy:} \quad f_3(X) = \max_{t>5} \left| \dot{H}(t) - \dot{H}_c \right| \tag{11}$$

The error between the attack angle and the attack angle command is defined as:

$$\text{Angle of attack error:} \quad f_4(X) = \int_{t>5} \left| \alpha(t) - \alpha_c \right| \tag{12}$$

To avoid the overreaction of the stabilator, the integration of the stabilator command δ_s is also added to the cost function:

$$\text{Stabilator command constraint:} \quad f_5(X) = \int_{t>0} |\delta_s| \tag{13}$$

As we can see, the control parameter optimization is a multi-objective optimization problem. In this paper, we use the weighting method to solve this problem. The five objective functions defined above are combined into one cost function using different weighting factors:

$$f(X) = w_1 f_1(X) + w_2 f_2(X) + w_3 f_3(X) + w_4 f_4(X) + w_5 f_5(X) \tag{14}$$

5. Simulation results and analysis

5.1. Results on benchmark functions

To test the performance of our modification to the basic BSO, we apply SBSO to a set of benchmark functions. The parameters used in BSO and SBSO are given in Table 1. We select eight benchmark functions to test our algorithm, four of them are unimodal functions, the other four are multimodal functions, as is shown in Table 2. The dimensions of the benchmark function are all 30.

The optimization results of BSO and SBSO in 30 runs are given in Table 3, and the comparisons of the evolutionary curves of the cost function are shown in Fig. 6. From Fig. 6 we can see that, SBSO convergences faster than the basic BSO obviously in the early stage, which coincides with our expectations. From Table 3 we are happy to see that, the accuracy of SBSO is also better than the basic BSO, which exceeds our expectations. This may indicate that adding noise to the combination of two ideas is more effective than adding noise to one idea.

5.2. Results on ACLS control parameter optimization problem

As is explained in Section 4.1, the inner loop shown in Fig. 1 is optimized by fitting the frequency response curve of the closed-loop system with a desired frequency response curve. The parameters to be optimized are $X = [K_{qm}, K_{qc}, T]$, the cost function used here is defined in Eq. (7).

The maximum iteration is set to 50. The frequency response of the optimized inner loop is shown in Fig. 7. The pitch rate

Table 2
Benchmark functions.

Functions	Type	Expressions	d	Range
Sphere	unimodal	$f_1 = \sum_{i=1}^{d} x_i^2$	30	$[-100, 100]$
Schwefel_P221	unimodal	$f_2 = \max\{\|x_i\|\}$	30	$[-100, 100]$
Schwefel_P222	unimodal	$f_3 = \sum_{i=1}^{d} \|x_i\| + \prod_{i=1}^{d} \|x_i\|$	30	$[-10, 10]$
Step	unimodal	$f_4 = \sum_{i=1}^{d} \|x_i + 0.5\|^2$	30	$[-100, 100]$
Rosenbrock	multimodal	$f_5 = \sum_{i=1}^{d-1} [100(x_{i+1} - x_i^2)^2 + (x_i - 1)^2]$	30	$[-30, 30]$
Ackley	multimodal	$f_6 = -20\exp(-0.2\sqrt{\frac{1}{d}\sum_{i=1}^{d} x_i^2}) - \exp(\frac{1}{d}\sum_{i=1}^{d}\cos(2\pi x_i)) + 20 + e$	30	$[-32, 32]$
Griewank	multimodal	$f_7 = \frac{1}{4000}\sum_{i=1}^{d} x_i^2 - \prod_{i=1}^{d}\cos(\frac{x_i}{\sqrt{i}}) + 1$	30	$[-600, 600]$
Schwefel_P226	multimodal	$f_8 = -\sum_{i=1}^{d}(x_i \sin(\sqrt{\|x_i\|})) + 418.9829d$	30	$[-500, 500]$

Table 3
Optimization results on benchmark functions in 30 runs.

Functions	BSO				SBSO			
	Min	Mean	Max	Std	Min	Mean	Max	Std
Sphere	5.71E−43	2.04E−28	6.12E−27	1.12E−27	1.60E−42	2.76E−42	4.00E−42	7.71E−43
Schwefel_P221	1.31E−02	2.04E+00	6.74E+00	1.84E+00	1.21E−02	2.21E−01	1.59E+00	3.28E−01
Schwefel_P222	3.27E−11	1.03E−05	1.18E−04	2.64E−05	9.20E−14	7.31E−07	8.69E−06	1.77E−06
Step	0.00E+00	0.00E+00	0.00E+00	0.00E+00	0.00E+00	0.00E+00	0.00E+00	0.00E+00
Rosenbrock	2.30E+01	4.85E+01	1.22E+02	3.09E+01	1.97E+01	3.16E+01	9.17E+01	1.88E+01
Ackley	7.11E−15	1.60E−14	3.20E−14	5.26E−15	3.55E−15	6.75E−15	7.11E−15	1.08E−15
Griewank	7.37E−13	1.30E−02	1.35E−01	2.51E−02	1.33E−15	3.29E−04	9.86E−03	1.80E−03
Schwefel_P226	3.82E−04	8.32E+00	1.18E+02	2.61E+01	3.82E−04	5.60E−01	1.68E+01	3.06E+00

response can be seen in Fig. 8. The optimization result is consistent with our expectation. The frequency response curve of the optimized system is similar to the desired frequency response curve.

We also use the handing quality to evaluate the performance of the optimized inner loop controller. Handling quality involves the study and evaluation of the stability and control characteristics of an aircraft. There are many ways to evaluate the handling quality, in this work, we use the Low-order Equivalent System (LOES) method. The aircraft model plus the inner loop controller is a high order system. First, we find the low-order equivalent system of the high-order equivalent system by frequency-domain fitting. Then we calculate the damping ratio ζ_{sp}, the inherent frequency ω_{sp} and the Control Anticipation Parameter (CAP) of the low-order equivalent system. CAP is defined as: the ratio of the initial pitch rate acceleration and the variation of the steady state normal overload:

$$\mathrm{CAP} = \ddot{\theta}_0 / \Delta n_{zss} = \omega_{sp}^2 / \left(n_z \cdot \alpha^{-1}\right) \tag{15}$$

Initially, we evaluate the CAP of the equivalent system, if CAP is between a certain range, it indicates that the aircraft is easy to maneuver. In Fig. 9, the horizontal axis is $(n_z \cdot \alpha^{-1})$ and the vertical coordinates is ω_{sp}, each pair of $(n_z \cdot \alpha^{-1}, \omega_{sp})$ determines a CAP. From Fig. 9 we can see that, the CAP of our control system is in Level 1 region. After we calculate CAP, ζ_{sp} and ω_{sp}, there are also several ways to evaluate the handling quality of the aircraft. The method we adopt in this work is directly using CAP and ζ_{sp}. In Fig. 10, the horizontal axis is ζ_{sp} and the vertical coordinate is CAP. We can see from Fig. 10 that out system satisfied Level 1 requirement.

As is explained in Section 4.2, after the inner loop is optimized, we again utilize SBSO to optimize the control parameters in the APCS and the autopilot. The control structures of the APCS and the autopilot can be seen in Fig. 2 and Fig. 3 respectively. The parameters to be optimized are $X = [K_{ai}, K_{ap}, K_{nz}, K_q, K_{\delta e}, K_{\dot{H}}, K_{\ddot{H}}, K_{\int \dot{H}}]$, and the cost functions used in the optimization problem are defined in Eq. (11) to Eq. (14). The weighting factors used in the cost function are: $w_1 = 5$, $w_2 = 5$, $w_3 = 150$, $w_4 = 1$, $w_5 = 1$. The optimization result is given in Table 3. A step H-dot command $\dot{H}_c = 5$ m/s is given to the autopilot, a constant attack angle variation reference $\Delta\alpha_c = 0°$ is given to APCS. The responses of vertical rate, attack angle and stabilator deflection are shown in Fig. 11 to Fig. 13 respectively. The evolutionary curve of SBSO is shown is Fig. 14. The results indicate the effectiveness of our method. The autopilot is able to track the H-dot command quickly and precisely. The settling time is around 5 s, and the overshoot is about 4.5%, which are similar to the design results in other literatures. The variation of attack angle is maintained at 0°. The deflection of the stabilator is acceptable.

6. Conclusions and future work

In this paper, we introduce an improved BSO, called SBSO. First, we apply both BSO and SBSO to a set of benchmark functions to demonstrate the effect of our improvement. Then, SBSO is applied to optimize the control parameters in the F/A-18A ACLS. The small turbulence longitudinal model of F/A-18A is considered. Our improvements simplify the procedure of BSO, and fewer parameters are required in the modified algorithm. The results on benchmark functions show that SBSO converges faster than the basic BSO, and the accuracy is also improved. The optimization result of ACLS shows that, our method is capable of optimizing the control parameters automatically both in the time domain and the frequency domain, and the result is satisfactory.

In the future, we will continue our research on utilizing bio-inspired algorithms to optimize the control parameters in flight control system. The method we introduced in this paper is a single-objective optimization method essentially. In dealing with the multi-objective optimization problem, we combine the objectives together using different weighting factors, however, the selection of the weighting factors is also difficult. In the future, we will turn to multi-objective optimization methods to solve the problem of optimizing the control parameters in ACLS.

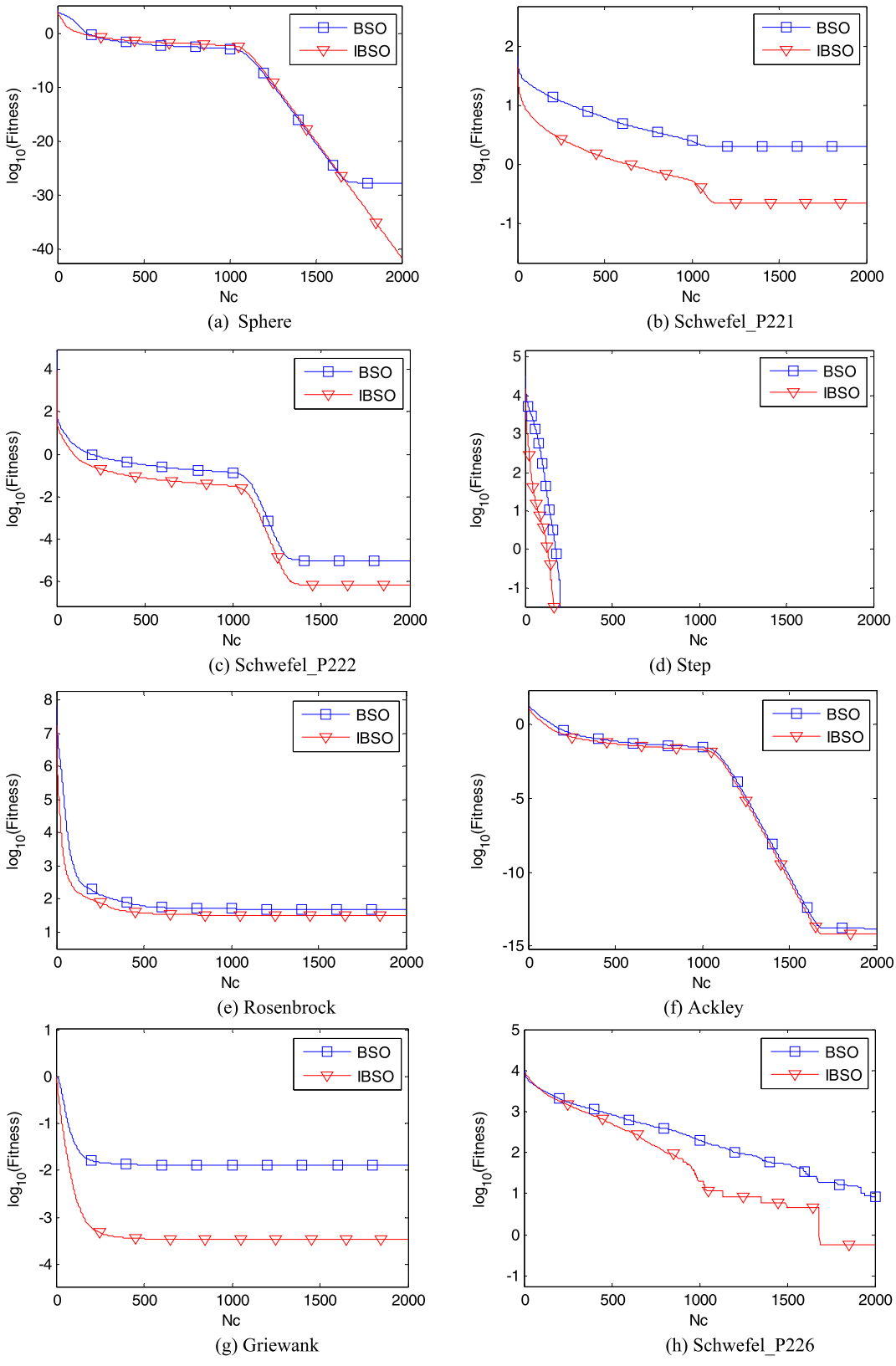

Fig. 6. Evolutionary curves of BSO and SBSO on benchmark functions.

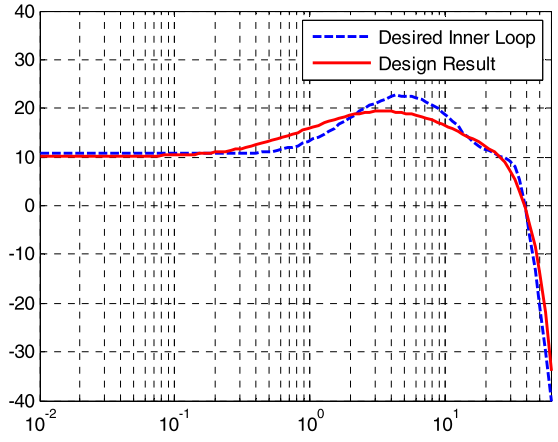

Fig. 7. Frequency response curve of the optimized inner loop.

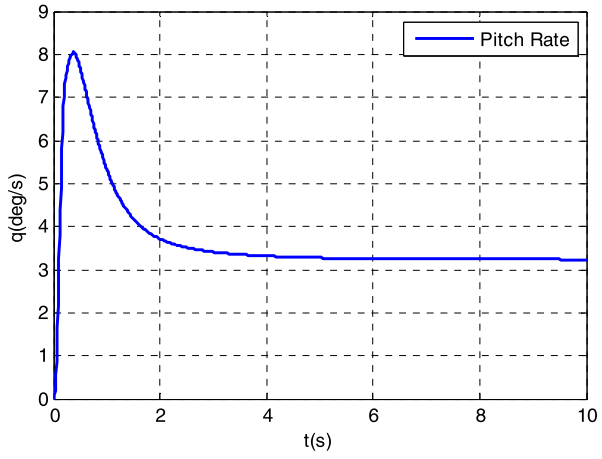

Fig. 8. Pitch rate response of the optimized inner loop.

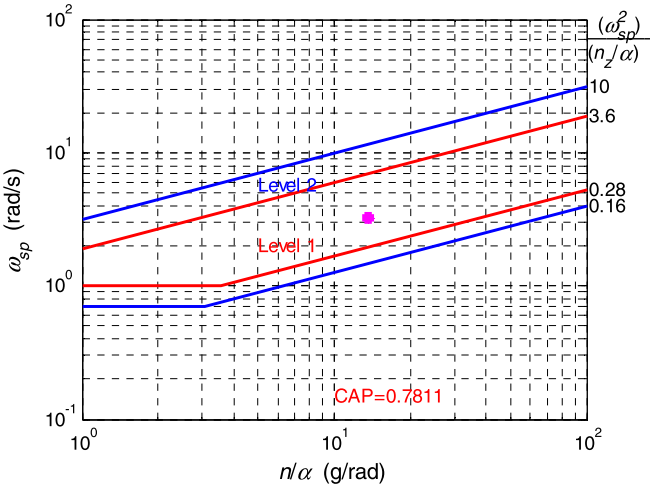

Fig. 10. Evaluation of the handing quality of the optimized inner loop.

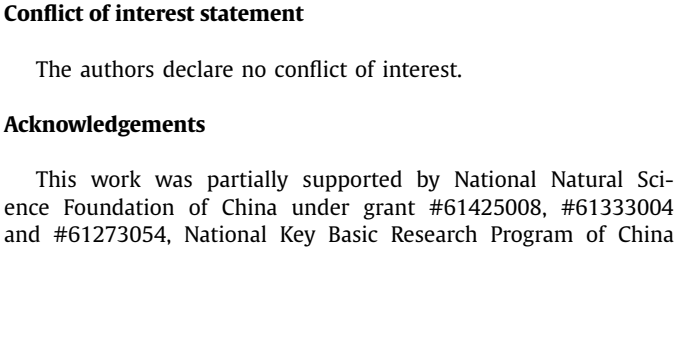

Fig. 9. Evaluation of the CAP of the optimized inner loop.

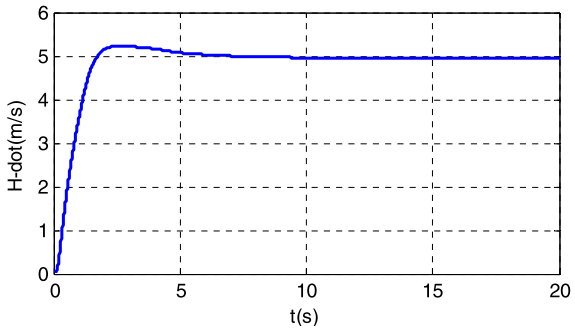

Fig. 11. Vertical rate response.

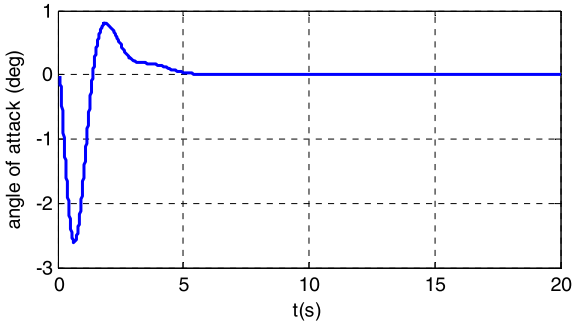

Fig. 12. Angle of attack response.

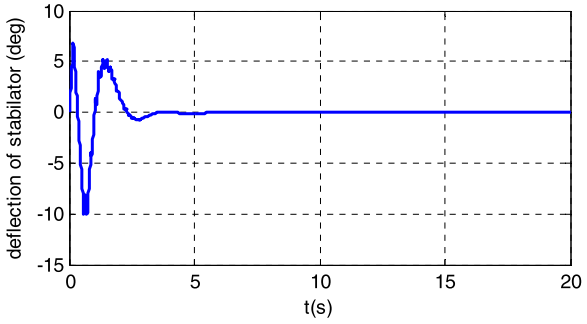

Fig. 13. Deflection of the stabilator.

Conflict of interest statement

The authors declare no conflict of interest.

Acknowledgements

This work was partially supported by National Natural Science Foundation of China under grant #61425008, #61333004 and #61273054, National Key Basic Research Program of China

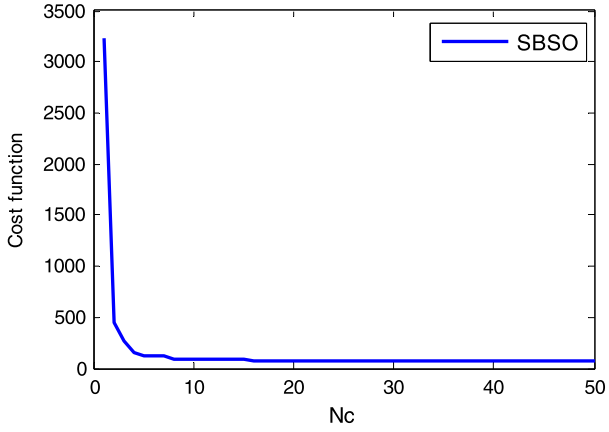

Fig. 14. Evolutionary curve of SBSO for the ACLS optimization problem.

(973 Project) under grant #2014CB046401, Top-Notch Young Talents Program of China, Aeronautical Foundation of China under grant #20135851042, and Graduate Innovation Foundation for Beihang University under grant #YCSJ-01-201405.

References

[1] B. Akay, D. Karaboga, A modified artificial bee colony algorithm for real-parameter optimization, Inf. Sci. 192 (2012) 120–142.
[2] T. Bäck, H.P. Schwefel, An overview of evolutionary algorithms for parameter optimization, Evol. Comput. 1 (1) (1993) 1–23.
[3] J. Brest, V. Zumer, M.S. Maucec, Self-adaptive differential evolution algorithm in constrained real-parameter optimization, in: Proceedings of 2006 IEEE Congress on Evolutionary Computation, Vancouver, BC, 16–21 Jul. 2006, IEEE, 2006, pp. 215–222.
[4] S. Cheng, Y. Shi, Q. Qin, Solution clustering analysis in brain storm optimization algorithm, in: Proceedings of 2013 IEEE Symposium on Swarm Intelligence, Singapore, 16–19 Apr. 2013, IEEE, 2013, pp. 111–118.
[5] S.J. Craig, R.F. Ringland, I.L. Ashkenas, An analysis of navy approach power compensator problems, J. Aircr. 9 (10) (1972) 737–743.
[6] J.L. Crassidis, D.J. Mook, Robust control design of an automatic carrier landing system, in: Proceedings of 1992 AIAA Astrodynamics Conference, Hilton Head Island, USA, 12–14 Aug. 1992, AIAA, 1992, pp. 1471–1481.
[7] H. Duan, C. Sun, Pendulum-like oscillation controller for micro aerial vehicle with ducted fan based on LQR and PSO, Sci. China, Technol. Sci. 56 (2) (2013) 423–429.
[8] H. Duan, S. Shao, B. Su, L. Zhang, New development thoughts on the bio-inspired intelligence based control for unmanned combat aerial vehicle, Sci. China, Technol. Sci. 53 (8) (2010) 2025–2031.
[9] H. Duan, S. Li, Y. Shi, Predator–prey Brain Storm Optimization for DC brushless motor, IEEE Trans. Magn. 49 (10) (2013) 5336–5340.
[10] H. Duan, Q. Luo, Y. Yu, Trophallaxis network control approach to formation flight of multiple unmanned aerial vehicles, Sci. China, Technol. Sci. 56 (5) (2013) 1066–1074.
[11] F. Gao, Y. Qi, Q. Yin, An novel optimal PID tuning and on-line tuning based on artificial bee colony algorithm, in: Proceedings of IEEE international Conference on Computational Intelligence and Software Engineering, Wuhan, China, 10–12 Dec. 2010, IEEE, 2010, pp. 1–4.
[12] H. Jadhav, U. Sharma, J. Patel, Brain Storm Optimization algorithm based economic dispatch considering wind power, in: Proceedings of IEEE International Conference on Power and Energy, Kota Kinabalu, Malaysia, 2–5 Dec. 2012, IEEE, 2012, pp. 588–593.
[13] G. Johnson, B. Peterson, J. Taylor, C. McCarthy, Test results of F/A-18 autoland trials for aircraft carrier operations, in: Proceedings of IEEE Conference on Aerospace, vol. 3, Big Sky, MT, US, 10–17 Mar. 2001, IEEE, 2001, pp. 1283–1291.
[14] K. Krishnakumar, D.E. Goldberg, Control system optimization using genetic algorithms, J. Guid. Control Dyn. 15 (3) (1992) 735–740.
[15] P. Li, H. Duan, Path planning of unmanned aerial vehicle based on improved gravitational search algorithm, Sci. China, Technol. Sci. 55 (10) (2012) 2712–2719.
[16] G. Li, Q. Jia, J. Shi, The optimization of flight control system based on an improved evolutionary strategy and referenced model, in: Proceedings of IEEE Second International Conference on Intelligent Computation Technology and Automation, Changsha, Hunan, China, 10–11 Oct. 2009, IEEE, 2009, pp. 918–921.
[17] G. Looye, H.D. Joos, Design of autoland controller functions with multi-objective optimization, in: Proceedings of AIAA Guidance, Navigation, and Control Conference and Exhibit, Monterey, California, 5–8 Aug. 2002.
[18] Q. Luo, H. Duan, An improved artificial physics approach to multiple UAVs/UGVs heterogeneous coordination, Sci. China, Technol. Sci. 56 (10) (2013) 2473–2479.
[19] P. Miotto, J.D. Paduano, E. Feron, Modern fixed structure control design, part I: gain adjustment to improve handling qualities, in: AIAA Guidance, Navigation and Control Conference, New Orleans, LA, USA, 1997, pp. 144–154.
[20] A.L. Prickett, C.J. Parkes, Flight testing of the F/A-18E/F automatic carrier landing system, in: Proceedings of IEEE Conference on Aerospace, vol. 5, Big Sky, MT, US, 10–17 Mar. 2001, IEEE, 2001, pp. 2593–2612.
[21] H. Qiu, H. Duan, Receding horizon control for multiple UAV formation flight based on modified Brain Storm Optimization, Nonlinear Dyn. 78 (3) (2014) 1973–1988.
[22] Y. Shi, Brain storm optimization algorithm, in: Proceedings of the 2nd International Conference on Swarm Intelligence, Chongqing, China, 12–15 Jun. 2011, Springer, 2011, pp. 303–309.
[23] Y. Shi, An optimization algorithm based on brainstorming process, Int. J. Swarm Intell. Res. 2 (4) (2011) 35–62.
[24] M.L. Steinberg, Development and simulation of an F/A-18 fuzzy logic automatic carrier landing system, in: Proceedings of the Second IEEE International Conference on Fuzzy Systems, Warminster, USA, Mar. 28–Apr. 1 1993, pp. 797–802.
[25] M.L. Steinberg, A.B. Page, A comparison of neural, fuzzy, evolutionary, and adaptive approaches for carrier landing, in: Proceedings of the AIAA Guidance, Navigation, and Control Conference and Exhibit, Montreal, Canada, 6–9 Aug. 2001.
[26] M.B. Subrahmanyam, H-infinity design of F/A-18A automatic carrier landing system, J. Guid. Control Dyn. 17 (1) (1994) 187–191.
[27] R. Sun, G. Chen, C. Zhou, Multidisciplinary design optimization of adaptive wing leading edge, Sci. China, Technol. Sci. 56 (7) (2013) 1790–1797.
[28] C. Sun, H. Duan, Y. Shi, Optimal satellite formation reconfiguration based on closed-loop brain storm optimization, IEEE Comput. Intell. Mag. 8 (4) (2013) 39–51.
[29] J.M. Urnes, R.K. Hess, Development of the F/A-18A automatic carrier landing system, J. Guid. Control Dyn. 8 (3) (1985) 289–295.
[30] J.M. Urnes, R.K. Hess, R.F. Moomaw, R.W. Huff, H-Dot automatic carrier landing system for approach control in turbulence, J. Guid. Control Dyn. 4 (2) (1981) 177–183.
[31] Z. Zhan, J. Zhang, Y. Shi, H. Liu, A modified brain storm optimization, in: Proceedings of 2012 IEEE Congress on Evolutionary Computation, Brisbane, Australia, 10–15 Jun. 2012, IEEE, 2012, pp. 1–8.
[32] Z. Zhan, W. Chen, Y. Lin, Parameter investigation in brain storm optimization, in: Proceedings of 2013 IEEE Symposium on Swarm Intelligence, Singapore, 16–19 Apr. 2013, IEEE, 2013, pp. 103–110.
[33] D. Zhou, Y. Shi, S. Cheng, Brain storm optimization algorithm with modified step-size and individual generation, Adv. Swarm Intell. 7331 (2012) 243–252.
[34] Q. Zhu, T. Wang, W. Zhang, F. Zhou, Variable structure approach power compensation system design of an automatic carrier landing system, in: Proceedings of 2009 IEEE Chinese Control and Decision Conference, Guilin, China, 17–19 June 2009, IEEE, 2009, pp. 5517–5521.